Superparamagnetic Latex Synthesized by a New Route of Emulsifier-Free Emulsion Polymerization

Seda Beyaz,[1] Taner Tanrisever,[1] Hakan Kockar,[2] Vural Butun[3]

[1]*Department of Chemistry, Balikesir University, Balikesir 10145, Turkey*
[2]*Department of Physics, Balikesir University, Balikesir 10145, Turkey*
[3]*Department of Chemistry, Eskisehir Osmangazi University, Eskisehir 26480, Turkey*

Received 2 May 2010; accepted 29 November 2010
DOI 10.1002/app.33895
Published online 16 March 2011 in Wiley Online Library (wileyonlinelibrary.com).

ABSTRACT: The aim of this study was to design polymeric nanospheres containing magnetic nanoparticle which could display superparamagnetic behavior and thus find application in allied fields. First magnetite nanoparticles were synthesized with coprecipitation method and then their stable acidic dispersion was prepared without surfactant and dropped into the polymerization system during a certain time interval after the polymerization started. The effects of time at which the magnetic sol was added into polymerization system on latex size and stability, average molecular weight of polymer were examined in the case of two different monomer concentrations. Extensive characterization by transmission electron microscopy, dynamic light scattering, thermal gravimetric analysis and magnetic measurements shows that when the magnetic sol was dropped during earlier time of polymerization at stage 1, the latex size, average molecular weight of polymer, thermal stability of polymeric composite, and saturation magnetization reduced, whereas polydispersity of size and molecular weight increased because of the reaction between persulfate and naked surface of magnetite at the aqueous phase. © 2011 Wiley Periodicals, Inc. J Appl Polym Sci 121: 2264–2272, 2011

Key words: superparamagnetic latex; emulsion polymerization; magnetite; emulsifier-free

INTRODUCTION

In the past decades, there has been great interest in the preparation of superparamagnetic latex because of many versatile applications[1,2] such as drug-delivery systems,[3] biosensors,[4] affinity separations,[5] and enzyme immobilizations.[6] Fe_3O_4 (magnetite), the dominant magnetic material in preparations of magnetic polymer nanospheres due to showing rather low toxicity and it can be synthesized through the coprecipitation of Fe(II) and Fe(III) salts by addition of a base.[7] The stabilization of magnetite nanoparticles (called magnetic fluid) in water can be achieved by two ways. First one is the magnetic fluids which are stabilized entirely by electrostatic repulsion and were introduced by Massart.[8] Second, the stabilization can be succeeded by coating the particle surface with bilayer surfactants.[9] A commonly used method for preparing magnetic polymer nanospheres is to suspend magnetic particles in the liquid phase of a polymerizable formulation and polymerize the monomer in the presence of the magnetic particles to form magnetic polymer nanospheres, including suspension,[10] miniemulsion,[11] and dispersion polymerization.[12] However, it is difficult to disperse hydrophilic magnetite particles into droplets of hydrophobic monomers by those processes based on direct monomer polymerization. Therefore, various materials such as emulsifier agents, co-surfactants, and long chain alcohols which have contaminated magnetic latex are used to eliminate this difficult. After the polymerization, the stabilizer, which covers the surface of the polymer nanospheres, may inhibit the performance of the magnetic nanoparticles or severely reduce the effectiveness of the particles.

Recently, the emulsifier-free emulsion polymerization which allows preparing highly monodisperse and "clean" latex was thought as suitable a way in preparing monodisperse magnetic polymer nanosphere. Furthermore, the emulsifier-free emulsions with well-defined surface properties are often used as model system to study rheology of colloids and support materials for biomolecules. Wang et al.[13] prepared magnetic poly(methyl methacrylate) (PMMA) nanospheres by emulsifier-free emulsion polymerization in the presence of ferrofluid with dodecanoic acid. The effects of various polymerization parameters, such as the monomer concentration, ferrofluid content, and initiator concentration, on the

Correspondence to: S. Beyaz (sedacan@balikesir.edu.tr).
Contract grant sponsor: Balikesir University, Turkey; contract grant number: BAP 2006/46.
Contract grant sponsor: State Planning Organisation, Turkey; contract grant number: 2005K120170.

conversion curve and particle size of the magnetic composite latex particles were examined in detail. The results showed that two nucleation mechanisms were involved because of emulsifiers along with magnetite nanoparticles. Pich et al.[14] first reported deposition of magnetite on highly monodisperse poly(styrene/acetoacetoxyethyl methacrylate) (PS-AAEM) nanoparticle synthesized by emulsifier-free emulsion polymerization. Second, they presented the synthesis of magnetic PS-AAEM nanospheres at various polymerization recipes included ferrofluid.[15] Xie et al.[16] examined the emulsifier-free emulsion polymerization of styrene–butyl acrylate–methacrylic acid in a polar solvent. No matter what synthesis methods are used, the polar surfaces of magnetite nanoparticles were modified by an emulsifier before they have been put into polymerization medium. This aspect has caused to reduce the magnetic separation capability of polymeric nanospheres as well as form " no clean" latex.

An important attraction of the inclusion of nanoparticles during polymer formation is the avoidance of extra reaction steps leading to simple production and scale-up. The proposed method in this study could have many advantages. The magnetic nanoparticles are simply added as a component during the polymerization process. There is no need to modify surfaces of the nanoparticles. The use of conventional polymerization stabilizers is avoided as these could negate the properties of the nanoparticles. There are also no byproducts produced in the process and no unwanted contaminants are left in the polymer.

In this article, which is first series in explaining the route, it has been examined the effects of time at which magnetic sol was put into polymerization system on the properties of superparamagnetic polymeric nanospheres. Uniform and separate distribution of magnetite nanoparticles inside polymeric nanospheres was observed and high M_s value was obtained, which provides wonderful advantages for diverse applications.

EXPERIMENTAL DETAILS

Materials

Methyl methacrylate (MMA), purchased from Merck, was freed from phenolic inhibitors by shaking with 5% (w/v) aqueous NaOH, washing with water, and drying over Na_2SO_4. The initiator, potassium persulphate (KPS), was a product of Fluka, Germany. Ferric chloride hexahydrate ($FeCl_3 \cdot 6H_2O$, purity: >99%), aqueous ammonia (25% NH_3 in water, w/w), perchloric acid ($HClO_4$, 60%, w/w) were obtained from Merck. Ferrous chloride tetrahydrate ($FeCl_2 \cdot 4H_2O$, purity: >99%) were purchased from Fluka. Double distilled water was used in all the stages of the workup. The conductivity of water was measured about 1.0–1.5 $\mu s\ cm^{-1}$ at 25°C.

Preparation of magnetic nanoparticles and magnetic sol

A total of 40 mL of 1*M* $FeCl_3 \cdot 6H_2O$ solution in water was combined with a 10 mL solution of 2*M* $FeCl_2 \cdot 4H_2O$ in 2*M* HCl. The chloride solutions were prepared quickly and added to 500 mL of 0.7*M* NH_4OH (purged initially with N_2 gas for 1 h before adding salts) in an open vessel. Thus, the following reaction was carried out at 1800 rpm for 30 min under a continuous flow of N_2.

$$2FeCl_3 + FeCl_2 + 8NH_4OH \rightarrow Fe_3O_4 + 8NH_4Cl + 4H_2O \quad (1)$$

According to reaction given above, magnetite precipitate formed and it was deposited with a magnet placed under the vessel of the solution, and supernatant liquid was removed. To remove probably unreacted chemicals and byproducts that were formed during the process; the precipitate was washed with double distilled water. Thereafter, it was stirred with aqueous 2*M* $HClO_4$ and was then isolated by centrifugation. After this process was repeated twice, the preparation of magnetic sol was accomplished merely by adding water.

Synthesis of poly(methyl methacrylate) nanospheres containing magnetic nanoparticles

The polymerization was carried out at 75°C in a 1-L round-bottomed four-necked glass flask equipped with a mechanical stirrer, nitrogen inlet, thermometer (±0.1°C), and condenser. The reactor was immersed in a thermostated water bath to maintain constant temperature. First, 900 mL of water and the defined amount of MMA were charged into the reactor and stirred under nitrogen atmosphere for about 60 min to remove oxygen from the reaction system. Temperature equilibrium was attained and the aqueous phase was saturated with monomer. The initiator, 0.51 g of KPS dissolved in 50 mL water, was added into the reactor. The magnetic sol was slowly dropped into polymerization system at the certain time interval straight after the polymerization started as simulated in Figure 4. Polymerization was carried to at 300 rpm for about 90 min.

Characterizations

The crystalline structure of magnetic nanoparticles was investigated with PANalytical's X'Pert PRO X-ray diffractometer system (XRD). The XRD patterns

were taken from 20° to 80° (2θ value) using CuKα radiation at room temperature. The particle size and size distribution of magnetite nanoparticles in magnetic sol were measured using an ALV/CGS-3 compact goniometer system (Malvern, UK). Total iron concentration in magnetic sol was determined spectrophotometrically after HCl/H_2O_2 induced oxidation Fe^{+2} to Fe^{+3} and addition of potassium thiocyanate followed absorption measurement of the thiocyanate complex at = 480 nm.[17] High-resolution transmission electron microscope (HRTEM, FEI TECNAI G^2 F30 model) with an accelerating voltage of 300 kV was used to obtain information about the morphology and size of the nanoparticles. Samples for HRTEM were prepared by placing a drop of very dilute magnetic dispersion on a copper grid covered by Formvar foil and drying.

To determine amount of free magnetite particles from the polymer particles, magnetic polymeric nanospheres were introduced into aqueous HCl solution (2*M*) in volumetric flask for 48 h at room temperature. After the suspension was centrifuged, the upper fraction was restrained for chemical analysis with thiocyanate described above. For hydrodynamic radius (R_H) and the polydispersity index (PDI) of magnetic polymeric nanospheres, dynamic light scattering (DLS) studies were conducted using Zetasizer NanoZS (Malvern Instruments). Before measurement, the latex particles were highly diluted; thereafter, the samples were introduced into a thermostated scattering cell at 25°C. Thermogravimetric analysis (TGA) with diamond series from PerkinElmer Instruments was used to observe thermal degradation behavior and the weight loss of composite samples. Approximately 10 mg of sample was placed in an aluminum pan and heated from 25 to 600°C at 20°C/min. To determine the average molecular weight (M_w) and polydispersity index (M_w/M_n) of polymers using gel permeation chromatography (GPC), it needs to separate magnetic nanoparticles from the polymers. For this, the dried polymeric composite samples were dissolved in the chloroform and iron powder was added to this solution. The magnetic nanoparticles in the solution adsorbed on the surface of the iron powder due to the effect of the magnetic field produced by a magnet put under the vessel of the solution at about 5 h. Thus, the polymers suspended while precipitating the magnetite in the chloroform and the polymer solution was separated by decanting. After the chloroform was removed, the dried polymers were dispersed in GPC eluent. The GPC consisted of an Agilent Iso Pump, a refractive index detector, both Mixed "D" and Mixed "E" columns (ex. Polymer Labs), and calibration was carried out using PMMA calibration standards. The GPC eluent was HPLC grade THF stabilized with BHT, at a flow rate of 1.0 mL/min. A vibrating-sample magnetometer (VSM-ADE EV9 Model) was used at room temperature to measure the magnetite nanoparticles and magnetic latex.

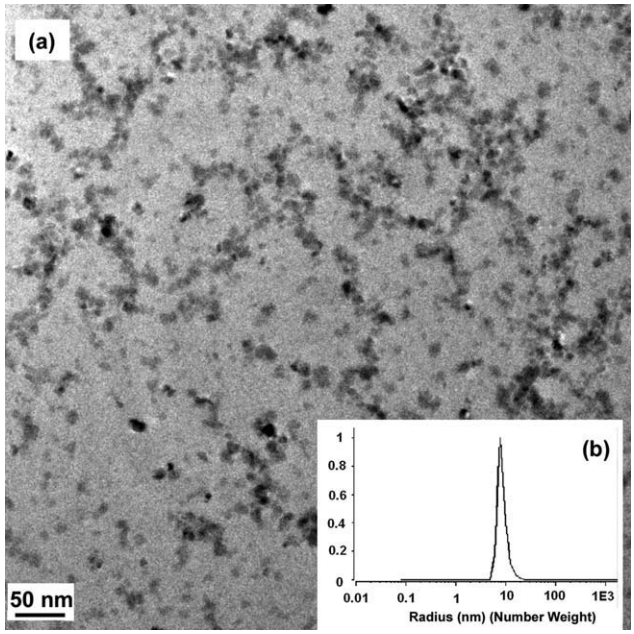

Figure 1 (a) HRTEM micrograph and (b) DLS diagram for as-synthesized magnetic nanoparticles

RESULTS AND DISCUSSION

Magnetic nanoparticles

The suspension of the black magnetite nanoparticles in the reaction solution was not stable and a precipitate had formed within a few minutes after synthesis. The aqueous colloidal suspension of magnetite nanoparticles (magnetic sol) treated by $HClO_4$ was stable for months. A dry powder of $HClO_4$-treated magnetic nanoparticles was used for XRD and VSM analysis, but did not form stable colloids with adding water again. Thus, the magnetic nanoparticles had been stored in acidic solution with a pH $\cong$ 2 during experiments. The concentration of magnetite inside the magnetic sol used at the polymerization was found as 3.51×10^{-2} g/mL by spectrophotometric method.[17]

HRTEM image and DLS diagram (see inset) in Figure 1 revealed that the magnetite nanoparticles were independently dispersed and thus they have the narrow size distribution in the magnetic sol. R_H and PDI of magnetic nanoparticles was measured 16.6 nm and 0.234 by DLS. Additionally, the mean particle diameter (d_p) and standard deviation (σ_g) was calculated as 9.57 nm and 2.25, respectively, by fitting log-normal distribution function[18] from HRTEM. It is worth noting that the value for the particle diameter obtained from electron microscopy means the particle core size, whereas the size detected using DLS system refers to a hydrodynamic diameter of particles.

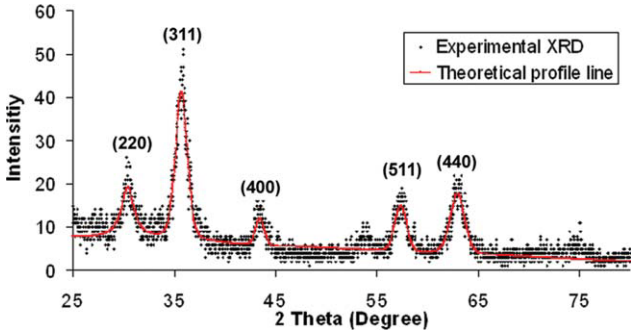

Figure 2 XRD pattern and the fit profile line of synthesized magnetic nanoparticles. [Color figure can be viewed in the online issue, which is available at wileyonlinelibrary.com.]

HRTEM also showed that the shapes of nanoparticles were not uniform as reported many times.[19,20]

The XRD pattern of magnetic nanoparticles showed a spinal phase in Figure 2. The precision of the XRD patterns was relatively low due to line broadening of nanocrystals.[21] The line positions and relative intensities were consistent with the presence of either magnetite or maghemite. However, sufficient minor differences of the XRD patterns of magnetite and maghemite, such as an absence of 210 and 213 lines of maghemite, indicate that a separated maghemite phase is not present.[22] On the basis of the Scherrer equation,[23] the average crystallite size for magnetite can be estimate using the half-maximum width of the most intense peak. However, because the assumption of an underlying crystal structure (translational symmetry) is often invalid,[24] it was preferred that diffraction profile was fitted by Pseudo-Voight function[25] for 5 peaks (220, 311, 400, 511, and 440). The line profile, shown in Figure 2, was obtained using XFit program[26] and the average crystal size was calculated as 9.62 ± 1.08 nm, which is consistent with HRTEM.

The hysteresis curve of the magnetite nanoparticles are illustrated in Figure 3. The saturation magnetization (M_s) was found to be equal to 50 emu/g at 300 K. As seen in the inset of magnetite nanoparticles, the typical characteristics of superparamagnetic behavior are observed showing zero coercivity and remanence. The magnetic particle size and the standard deviation can also be calculated from the fitting of the hysteresis curve[27] as 9.15 nm and ±0.37, which is smaller than that observed from XRD and HRTEM measurement. The reason of small magnetic size has been reported that the surface layer of magnetite atoms does not contribute to the magnetic properties of the particle.[28]

Superparamagnetic latex polymerization mechanism

In the first stage of polymerization, the solubility of the monomer increases because of the addition of

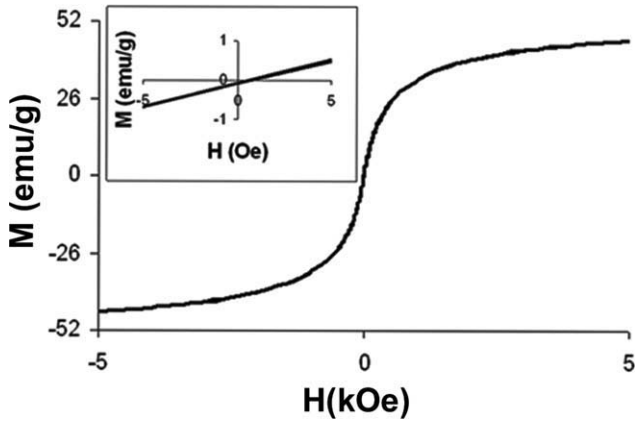

Figure 3 Magnetization curve of synthesized magnetite nanoparticles, inset shows zero coercivity.

the polar sulfate group, but then decreases as the chain length grows. The chain propagation of oligomer free radicals would eventually become insoluble. Shorter chain oligomers and monomer would be preferentially incorporated into this structure and therefore leading to the formation of particles. Furthermore, the smaller particles would coagulate to form larger particles until the potential energy of electrostatic repulsion between the particles is adequate to ensure colloid stability in the ionic environment in which the primary particle is formed.[29] Meanwhile, the polymerization rate increases with decreasing termination reactions and the conversion of polymerization goes up suddenly[30–32] as simulated in Figure 4. If the magnetic nanoparticles are added to polymerization reactor

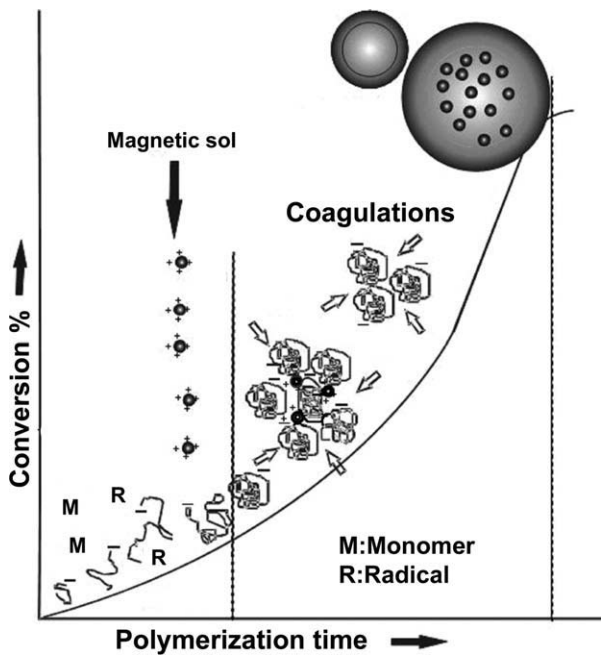

Figure 4 The simulation of theoretical approach used in synthesis of superparamagnetic latex.

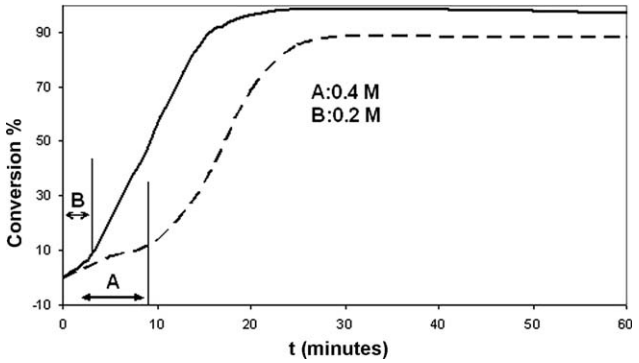

Figure 5 The conversion curves of sample 1A (----) and sample 1B (__) at the emulsifier-free, emulsion polymerization system.

shortly before coagulation, they can embed in polymeric chains or nanospheres (see Fig. 4) during coagulation. Besides, the magnetic nanoparticles separately can settle inside polymeric nanospheres not aggregating and thus the superparamagnetic property can converse.

From this point of view, first, we have investigated the conversion curve of polymerization to find suitable time at which magnetic nanoparticles were added as seen Figure 5. As expected,[33] the increase of monomer concentration caused to extend time interval of Stage 1. Thus, the magnetic sol was dropped until 5.5 min of polymerization in the end of Stage 1 for 0.2*M* concentration of monomer, whereas it was selected as 7.5 min for 0.4*M* monomer.

Superparamagnetic latexes

Superparamagnetic PMMA latexes were synthesized successfully by a new direct route based emulsifier-free emulsion polymerization. The experimental conditions used in the synthesis, and size, average molecular weight of polymer, and magnetic properties of latexes were shown in Table I.

The magnetite inside polymeric nanospheres was not dissolved visually in 2*M* HCl for several days, whereas free magnetite particles were completely dissolved within a day, which means that latex is though to include magnetite nanoparticles. In addition, to clarify, direct observations of the magnetic latex carried out by using HRTEM showed that the magnetite nanoparticles within the polymer spheres are easily identified in the HRTEM photography, as seen in Figure 6(A). The electron diffraction model in Figure 6(B) confirmed that the black particles within polymeric nanosphere are magnetite crystals.

Although the results indicated that the magnetite nanoparticles were effectively covered by the polymer matrix, for more accurate an investigation, the aqueous HCl solution of magnetic polymeric nanospheres that was kept for 48 h was centrifuged, and the upper fraction was restrained for chemical analysis with thiocyanate[17] and the amount of free magnetite nanoparticles from the polymer particles were determined. Figure 7 shows factors affecting percentage of magnetite inside polymeric nanosphere. During the polymerization process with 0.4*M* monomer concentration, it was noticed the big brown particles (called aggregate) in the polymerization reactor. In the case of the high aggregate, it was found that magnetite percentage inside polymeric nanosphere decreased as seen Figure 7. Thereafter, it was aimed to synthesis latex not including aggregation. The aggregate amount increased when magnetic sol was added at early minutes (1–2.5 min) of polymerization. The least aggregate amount was obtained with adding magnetic sol at 2.5–5 min of polymerization. However, it was always observed the aggregates at 0.4*M* monomer concentration, even less magnetic sol was used as well Sample 5A, whereas there was no aggregate for 0.2*M* monomer concentration. This is probably due to decrease coagulation as a result of the increase of radical to monomer ratio. Through the research, latex which all of magnetite

TABLE I
The Properties of Synthesized Latexes and Experimental Conditions

Sample	Time interval (min)[a]	Magnetic sol (mL)	R_T (nm)	R_H (nm)	PDI	M_w(g /mol)	M_w /M_n	M_s (emu/g)
1A[b]	–	0	248 ± 09	249	0.002	–	–	–
2A	1–3.5	10	–	331	0.126	–	–	0.301
3A	2.5–5	10	301 ± 59	345	0.173	–	–	0.420
4A	5–7.5	10	320 ± 25	400	0.019	–	–	0.520
5A	2.5–5	5	–	376	0.130	–	–	0.091
1B[c]	–	0	–	223	0.009	113,450	1.84	–
2B	1–3.5	5[d]	196 ± 27	220	0.024	76,889	2.78	0.302
3B	2.5–5	5[d]	–	236	0.002	85,632	2.67	0.307
4B	3.5–5.5	5[d]	–	244	0.018	151,180	1.75	0.326

[a] The magnetic sol was dropped into polymerization medium.
[b] A series: 0.4*M* monomer.
[c] B series: 0.2*M* monomer, R_T is the particle size determined by electron microscopy.
[d] Magnetic sol was mixed 5-mL distilled water.

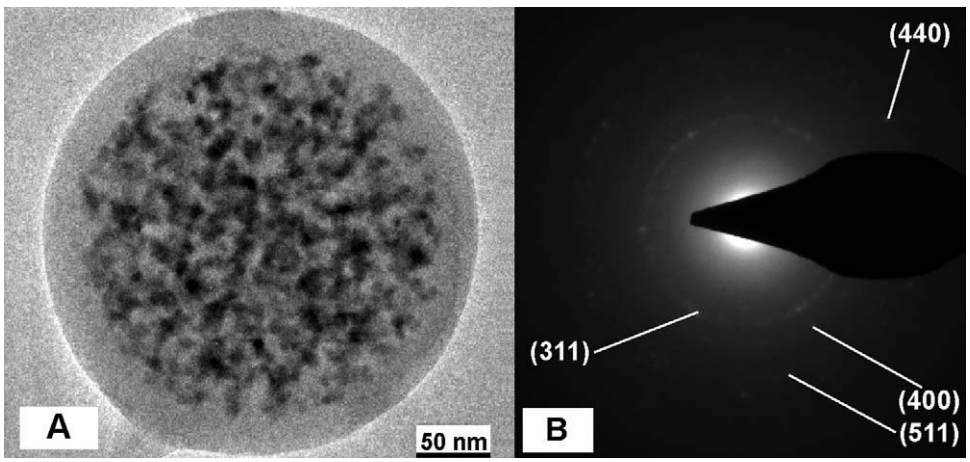

Figure 6 The uniform distribution of magnetic nanoparticles inside only one polymeric nanosphere (A) and its electron diffraction (B) by HRTEM.

nanoparticles were settled in polymeric nanospheres was determined as Sample 3B according to chemical analysis, see Figure 7.

Effect of time at which the magnetic sol was dropped into polymerization reactor

As shown in Table I, it is obvious that hydrodynamic radius of latex increases as start time to add magnetic sol delays for both monomer concentrations. This rise was more pronounced for 0.4*M* monomer concentration since much more magnetic sol was added and it was also confirmed by the result of electron microscopy, see Table I. The variation of the particle size may be attributed to the following reasons. Fe^{+2} ions on surface of magnetite nanoparticles can accelerate the decomposition of persulfate initiator and increase radical concentration as the reaction[34] (2).

$$Fe^{+2} + S_2O_8^{-2} \rightarrow SO_4^{-\bullet} + SO_4^{-2} + Fe^{+3} \qquad (2)$$

The reaction (2) formed in aqueous phase should be effective when the magnetic sol was added at the first minutes of polymerization because there are not enough polymeric species to coat on the surface of magnetic nanoparticles. Thus, naked magnetite nanoparticles act as radical source and cause a decrease in latex size. The particle size distribution (PDI) results obtained from DLS showed that PDI values were higher in the case of 0.4*M* monomer because of the aggregations. For both monomer concentrations, the adding of magnetic sol at earlier time of polymerization caused the increase of PDI value. To check DLS results, the electron micrographs of Samples 3A and 4A were taken by HRTEM. Indeed, as shown in Figure 8, it was found that the particle size distribution of Sample 3A that was synthesized with adding magnetic sol at the earlier times (2.5–5 min) of polymerization broader than the ones of Sample 4A (5–7.5 min). This is probably due to the increase of tendency to coalesce magnetic nanoparticles because the stabilizing effect of oligomeric molecules at earlier time of

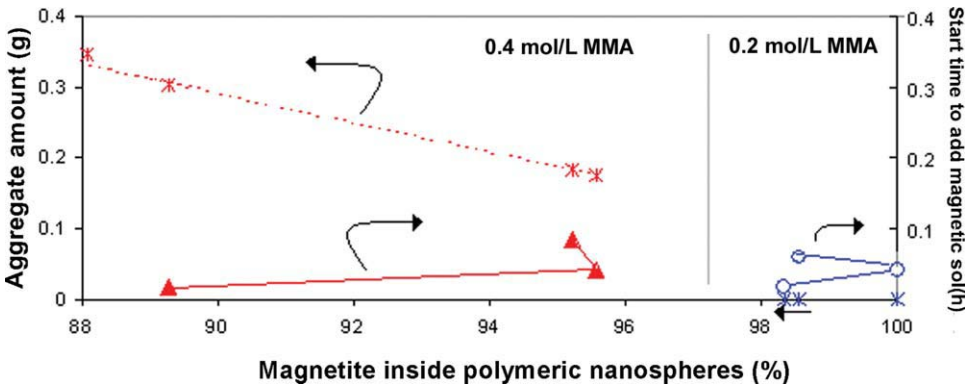

Figure 7 The effects of aggregate amount and the start time to add magnetic sol on the amount ofmagnetite inside polymeric nanospheres for both monomer concentration. [Color figure can be viewed in the online issue, which is available at wileyonlinelibrary.com.]

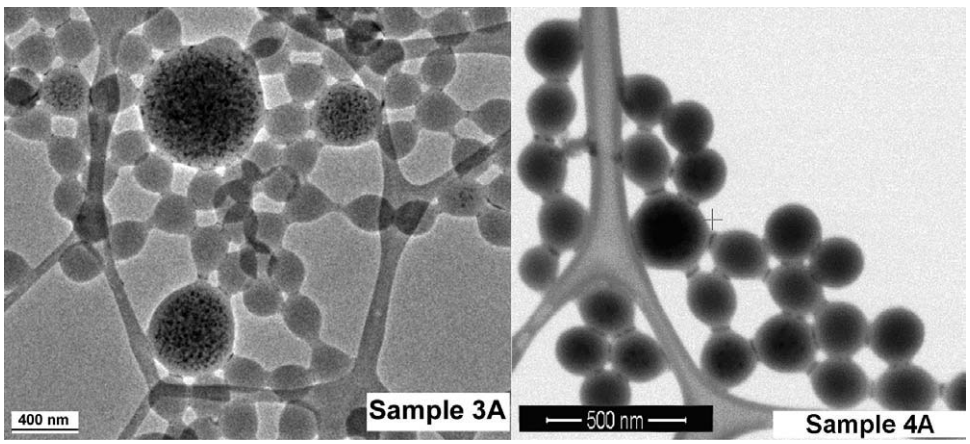

Figure 8 Electron microscopy pictures of Sample 3A and Sample 4A which were synthesized adding magnetic sol at 2.5-5 and 5-7.5 minutes of polymerization respectively.

polymerization was lower. It was also seen clearly from Figure 8 that the distribution of magnetic nanoparticles inside polymeric nanospheres at Sample 4A was more uniform than Sample 3A.

Table I also shows the polydispersity indexes and average molecular weights of PMMA synthesized using 0.2*M* of monomer, measured by GPC. With the magnetic sol was put on at the 1 min (Sample 2B) and 2.5 min (Sample 3B) of polymerization, the molecular weight of polymer reduced and polydispersity index increased if to compare with pure PMMA (Sample 1B) prepared at similar conditions. On the contrary, with the addition of magnetic sol was done at 3.5 min (Sample 4B) of polymerization, the molecular weight of polymer increased and polydispersity index decreased. In other words, it can be concluded that the later is the time to start adding of magnetic sol, the longer is polymeric chains. The reaction in (2) causes to increase radical concentration, leading to relatively the smaller molecular weight. However, the reaction occurs effectively at aqueous phase whose rate is higher at the first minutes of polymerization. Figure 9 presents a comparison of TGA curves for Samples 2A–4A. It was found that thermal stability of samples synthesized adding magnetic sol at the earlier time of polymerization is weak because of their low molecular weight.[35] Besides, magnetite content in polymeric composites for Samples 2A–4A was determined 0.767, 1.288, and 1.184 (%), respectively, although the same amount of magnetic sol was used due to aggregations.

Superparamagnetic natures of the synthesized magnetic PMMA latexes detected from the magnetization curve are presented in Figure 10. Neither remanence nor coercivity was observed as also seen in the inset of Figure 10. The M_s values obtained from the curve was collected in Table I, which are higher than that of other studies using emulsifier-free polymerization.[14,36] For example, Gu et al.[36] found $M_s = 0.5$ emu/g at 5% of magnetite: monomer ratio as initial mixture of polymerization, whereas we have obtained the same M_s value at 1.046%. Furthermore, in our polymerization system, the polymeric nanospheres not containing magnetic nanoparticles that are simultaneously formed can be easily separated from the magnetic polymeric nanospheres due to the effect of the magnetic field produced by a magnet placed under the vessel of the solution at about 5 hs. Therefore, M_s value of superparamagnetic polymeric nanospheres increased to about 10-fold.

Although the same amounts of magnetic sol were used, the different M_s values were observed. In the case of 0.4*M* monomer concentration, it can be said that aggregations caused this case, however for both monomer concentrations, it was noticed that M_s value increased as the start time to add magnetic sol was became later. This result confirmed eq. (2) that the magnetite was reacted with persulfate initiator

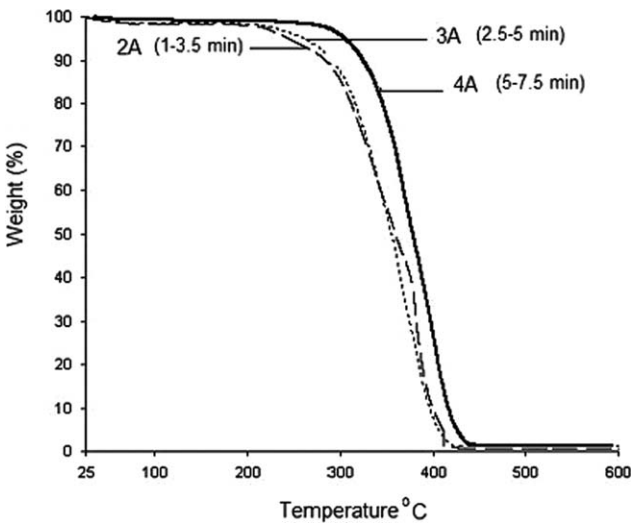

Figure 9 Thermal degration behavours of samples; 2A, 3A and 4A.

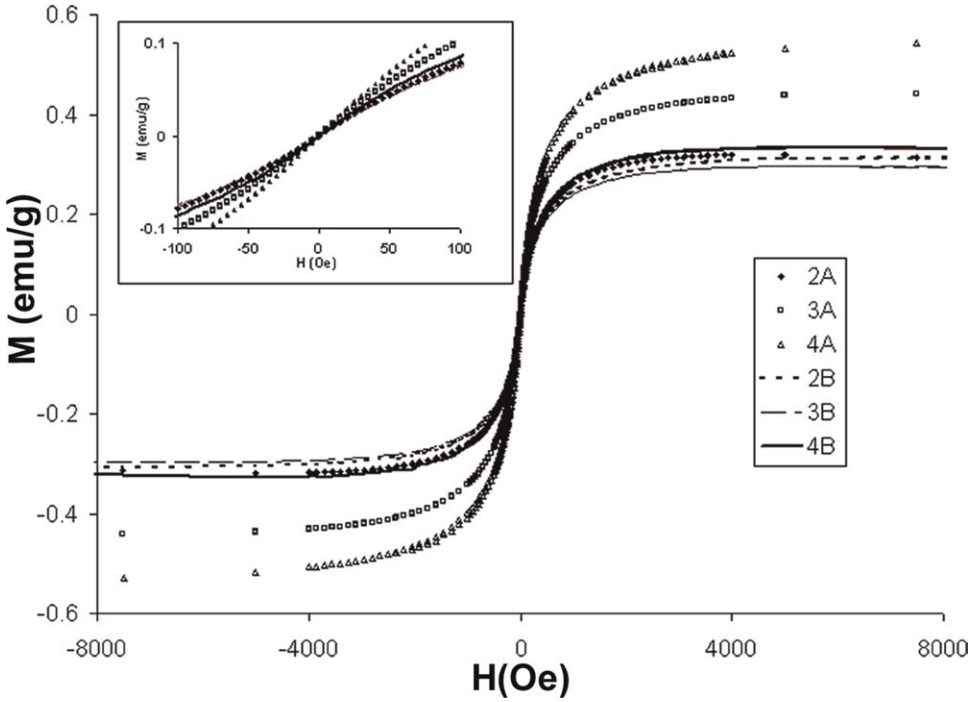

Figure 10 Hysteresis curves of as-synthesized PMMA nanocomposites. Inset shows zero coercivity that is a result of superparamagnetic property.

as mentioned in the part of latex size and molecular weight. Because of the reaction, the charge equilibrium at magnetite crystal can changes, an oxide layer can occur and as a result, the magnetic properties of nanoparticles can reduce.

CONCLUSIONS

The synthesis of superparamagnetic polymeric nanospheres can be efficiently achieved via a new direct route based emulsifier-free emulsion polymerization. During the new route, the surfaces of magnetic nanoparticles were not modified with any surfactant, as opposed to the literature. Electron microscopy characterization of magnetic latex particles show that ~9 nm of superparamagnetic magnetite particles were homogeneously loaded within the polymer nanospheres. The concentration of monomer and start time to add magnetic sol plays an important role in successful loading of magnetite nanoparticles and stability of latex. Persulfate initiator reacts with the magnetite nanoparticle, which leads to the formation of the smaller polymeric nanospheres and the shorter polymeric chains. Tough the magnetite content is not very high, magnetic response is found very fine. The magnetic polymer nanospheres were still superparamagnetic. These results indicate that these magnetic lattices will be promising for diverse applications.

The authors thank Dr. H. Guler for XRD analysis as well as Dr. M. Dogan and Y.Turhan for TGA analysis at Balikesir University, Turkey.

References

1. Tartaj, P.; Morales, M. P.; González-Carreno, T.; Veintemillas-Verdaguer, S.; Serna, C. J. J Magn Magn Mater 2005, 28, 290.
2. Mornet, S.; Vasseur, S.; Grasset, F.; Veverka, P.; Goglio, G.; Demourgues, A.; Portier, J.; Pollert, E.; Duguet, E. Prog Solid State Chem 2006, 34, 237.
3. Lübbe, A. S.; Alexiou, C.; Bergemann, C. J Surg Res 2001, 95, 200.
4. Meyer, M. H. F.; Stehr, M.; Bhuju, S.; Krause, H. J.; Hartmann, M.; Miethe, P.; Singh, M.; Keusgen, M. J Microbiol Methods 2007, 68, 218.
5. Li, Y. C.; Lin, Y. S.; Tsai, P. J.; Chen, C. T.; Chen, W. Y.; Chen, Y. C. Anal Chem 2007, 79, 7519.
6. Liao, M. H.; Chen, D. H. Biotechnol Lett 2001, 23, 1723.
7. Laurent, S.; Forge, D.; Port, M.; Roch, A.; Robic, C.; Elst, L. V.; Muller, R. N. Chem Rev 2008, 108, 2064.
8. Massart, R. IEEE Trans Magn 1981, 17, 1247.
9. Vekasi, L.; Bica, D.; Marinica, O. Rom Rep Phys 2006, 58, 257.
10. Cocker, T. M.; Fee, C. J.; Evans, R. A. Biotechnol Bioeng 1997, 53, 79.
11. Ramirez, L. P.; Landfester, K. Macromol Chem Phys 2003, 204, 22.
12. Horak, D. J Polym Sci Part A: Polym Chem 2001, 39, 3707.
13. Wang, P. C.; Chiu, W. Y.; Lee, C. F.; Young, T. H. J Polym Sci Part A: Polym Chem 2004, 42, 5695.
14. Pich, A.; Bhattacharya, S.; Adler, H. J. P. Polymer 2005, 46, 1077.
15. Pich, A.; Bhattacharya, S.; Ghosh, A.; Adler, H. J. P. Polymer 2005, 46, 4596.
16. Xie, G.; Zhang, Q.; Luo, Z.; Wu, M.; Li, T. J Appl Polym Sci 2003, 87, 1733.
17. Zaitsev, V. S.; Filimonov, D. S.; Presnyakov, I. A.; Gambino, R. J.; Chu, B. J Colloid Interface Sci 1999, 212, 49.
18. Ali-zade, R. A. Inorg Mater 2008, 44, 1105.
19. Liu, Z. L.; Liu, Y. J.; Yao, K. L.; Ding, Z. H.; Tao, J.; Wang, X. J Mater Synth Process 2002, 10, 83.

20. Nedkova, I.; Merodiiska, T.; Slavov, L.; Vandenberghe, R. E.; Kusano, Y.; Takada, J. J Magn Magn Mater 2006, 300, 358.
21. Scardi, P.; Leoni, M. Acta Crystallogr A 2001, 57, 604.
22. Schwertmann, U.; Cornell, M. R. Iron Oxides in the Laboratory Preparation and Characterization; VCH: New York, 1991.
23. Abdullah, M.; Khairurrijal, M. J Nano Saintek 2008, 1, 28.
24. Hall, B. D.; Zanchet, D.; Ugarte, D. J Appl Crystallogr 2000, 33, 1335.
25. Sanchez-Bajo, F.; Cumbrera, L. J Appl Crystallogr 1997, 30, 427.
26. Cheary, R. W.; Coelho, A. A. Software: Xfit-Koalariet CCP14 Library, 1996, http://www.ccp14.ac.uk.
27. Chen, D. X.; Sanchez, A.; Taboada, E.; Roig, A.; Sun, N.; Gu, H. C. J Appl Phys 2009, 105, 083924.
28. Kaiser, R.; Miskolczy, G. J Appl Phys 1970, 41, 1064.
29. Fitch, R. M. Br Polym J 1973, 5, 467.
30. Song, Z.; Poehlein, G. W. J. J Colloid Interface Sci 1989, 128, 486.
31. Arai, M.; Arai, K.; Saito, S. J Polym Sci Polym Chem Ed 1979, 17, 3655.
32. Aslamazova, T. R. Prog Org Coating 1995, 25, 109.
33. Tanrisever, T.; Okay, O.; Sonmezoglu, I. J Appl Polym Sci 1996, 61, 485.
34. Kolthoff, I. M.; Medalia, A. I.; Raaen, H. P. J Am Chem Soc 1951, 73, 1733.
35. McNeil, I. C. Eur Polym J 1968, 4, 21.
36. Gu, S.; Onishi, J.; Kobayashi, Y.; Nagao, D.; Konno, M. J Colloid Interface Sci 2005, 289, 419.